

## Dromion can be remote-controlled

This article has been downloaded from IOPscience. Please scroll down to see the full text article.

1998 J. Phys. A: Math. Gen. 31 3325

(<http://iopscience.iop.org/0305-4470/31/14/017>)

View [the table of contents for this issue](#), or go to the [journal homepage](#) for more

### Download details:

IP Address: 171.66.16.121

The article was downloaded on 02/06/2010 at 06:32

Please note that [terms and conditions apply](#).

## Dromion can be remote-controlled

Naoki Yoshida†¶, Katsuhiko Nishinari‡, Junkichi Satsuma§ and Kanji Abe||

† Department of Mechanics, Royal Institute of Technology, Osquars backe 18, 100-44 Stockholm, Sweden

‡ Department of Mechanical Engineering, Faculty of Engineering, Yamagata University, Jonan, 4-3-16, Yonezawa-shi, Yamagata 992, Japan

§ Department of Mathematical Sciences, University of Tokyo, Komaba 3-8-1, Meguro-ku, Tokyo 153, Japan

|| College of Arts and Sciences, University of Tokyo, Komaba 3-8-1, Meguro-ku, Tokyo 153, Japan

Received 20 October 1997

**Abstract.** The one-dromion solution of the Davey–Stewartson 1 equations with driving boundaries is analysed numerically. It is shown that the dromion can follow the motion of the crosspoint of the mean flows even if it is not of exact solutions. Moreover, it is found that the localized structure keeps its shape when it is exposed to the ‘forced’ motion of the mean flows. In the case where dromion runs on a circle path, the decay ratio of the localized structure versus the radius is given. Several types of movement of mean flows are also studied. It is expected that dromion can be controlled arbitrarily by driving mean flows at the boundaries.

### 1. Introduction

Recently the localized structure in the two-dimensional system described by the Davey–Stewartson (DS) 1 equations [1]

$$iA_t + A_{xx} + A_{yy} - 2|A|^2A + 2Q_xA = 0 \quad (1)$$

$$Q_{xx} - Q_{yy} = 2(|A|^2)_x \quad (2)$$

has been attracting a good deal of interest. The localized structure, called ‘dromion’ [2], has many interesting characteristics. For example, the variable  $A$ , hereafter called the main flow, is localized in two-dimensional space while the variable  $Q$ , hereafter called the mean flow, is not. Another interesting feature is that the mean flow is driven at the boundaries like a one-dimensional soliton [3]. We shall give exact formulae describing this boundary condition in section 2. Dromion exists under the interaction between the main flow and mean flows. This feature produces a stimulating question. Can dromion be controlled arbitrarily if we handle the mean flow boundaries?

Since the DS1 equations appear in several branches of physics, such as fluid dynamics [4] and plasma physics [5], these localized structures are worth being analysed in detail. So far collisions of dromions [6] and time evolution of one-dromion [7] have been studied numerically. Many other behaviours of dromions, however, still remain veiled. The purpose of this paper is to investigate in detail how dromions behave when we drive mean flows at

¶ On leave from: Department of Aeronautics and Astronautics, Faculty of Engineering, University of Tokyo, Hongo 7-3-1, Bunkyo-ku, Tokyo 113, Japan.

the boundary, that is, the position is forced to move in a certain way. In this situation it is expected that dromions follow the motion of the crosspoint of mean flows in view of the fact that the crosspoint plays a significant role as an attracting spot. We employ numerical computation to study the behaviour of dromions.

This paper is organized as follows. In section 2, we summarize the dromion solution of the DS1 equations. In section 3, we introduce another form of the DS1 equations and propose a new numerical scheme. Computational results are given in section 4. Concluding remarks are given in section 5.

## 2. The one-dromion solution

Let us summarize the one-dromion solution of the DS1 equations. In equations (1) and (2), making a  $45^\circ$  rotation in the coordinate space as  $x \rightarrow x + y$ ,  $y \rightarrow x - y$ , and introducing new variables,  $U \equiv Q_x - |A|^2$ ,  $V \equiv Q_y - |A|^2$ , we obtain

$$iA_t + A_{xx} + A_{yy} + (U + V)A = 0 \quad (3)$$

$$U_y = (|A|^2)_x \quad V_x = (|A|^2)_y. \quad (4)$$

The one-dromion solution is expressed as

$$A = \frac{\rho \exp(\eta_1 + \eta_2)}{1 + \exp(\eta_1 + \eta_1^*) + \exp(\eta_2 + \eta_2^*) + \gamma \exp(\eta_1 + \eta_1^* + \eta_2 + \eta_2^*)}. \quad (5)$$

In equation (5), parameters are given by

$$\begin{aligned} |\rho| &= 2\sqrt{2k_r l_r (\gamma - 1)} \\ \eta_1 &= (k_r + ik_i)x + (\Omega_r + i\Omega_i)t \\ \eta_2 &= (l_r + il_i)y + (\omega_r + i\omega_i)t \\ \Omega_r &= -2k_r k_i \quad \omega_r = -2l_r l_i \\ \Omega_i + \omega_i &= k_r^2 + k_i^2 + l_r^2 + l_i^2 \end{aligned}$$

where  $\gamma$ ,  $k_r$ ,  $k_i$ ,  $l_r$  and  $l_i$  are real constants. These five are substantially free parameters of the one-dromion solution. The constant  $\gamma$  determines an amplitude,  $k_r$  is the width of the pulse in the  $x$ -direction, and  $l_r$  in the  $y$ -direction. The quantities  $k_i$  and  $l_i$  are  $x$  and  $y$  components of velocity, respectively.

The potentials  $U$  and  $V$  are determined simply by integrating equation (4). For the dromion solution, boundary values of potentials  $U$  and  $V$  are not zeros, but are given in the form of one-dimensional soliton by

$$U|_{y=-\infty} = \frac{8k_r^2 \exp(\eta_1 + \eta_1^*)}{[1 + \exp(\eta_1 + \eta_1^*)]^2} \quad (6)$$

$$V|_{x=-\infty} = \frac{8l_r^2 \exp(\eta_2 + \eta_2^*)}{[1 + \exp(\eta_2 + \eta_2^*)]^2}. \quad (7)$$

One should be aware from equation (5) that the main flow  $A$  has a peak at the cross section of mean flows  $U$  and  $V$ , and that its peak decays exponentially in any direction in two-dimensional plane. Boundary conditions (6) and (7) play an important role on handling the one-dromion, which will be discussed in section 4.

### 3. Numerical scheme to solve the DS1 equations

As we see in equations (1) and (2), the time evolution of mean flow  $Q$  is not given explicitly. It is given nonlinearly and implicitly through the main flow  $A$ . This nature causes some difficulties in computation.

To make equation (2) easier to solve numerically, we split equation (2) into two first-order hyperbolic systems. We put

$$\hat{Q} = Q_x + Q_y. \quad (8)$$

Then equation (2) is written as

$$\hat{Q}_x - \hat{Q}_y = 2(|A|^2)_x \quad (9)$$

from which we obtain a conserved form

$$\hat{Q}_y - (\hat{Q} - 2|A|^2)_x = 0. \quad (10)$$

Next, by differentiating equation (8) by  $x$ , we obtain

$$(Q_x)_y + (Q_x - \hat{Q})_x = 0 \quad (11)$$

which is also in a conserved form.

Introducing an appropriate scale transformation and putting  $\hat{Q} = B$ ,  $Q_x = C$ , the DS1 equations (1) and (2) are rewritten as

$$iA_t + A_{xx} + A_{yy} + (2C - |A|^2)A = 0 \quad (12)$$

$$B_y - (B - |A|^2)_x = 0 \quad (13)$$

$$C_y + (C - B)_x = 0. \quad (14)$$

Although these equations look more complicated than the original ones, they are in a convenient form for numerical simulations.

Next we briefly explain the numerical method for solving the initial-boundary problem of the DS1 equations. If the main flow  $A$  is given at one moment and the outer boundary conditions  $B|_{y=-\infty}$  and  $C|_{y=-\infty}$  are designated.

(i) The wave equation (13) is solved from  $B|_{y=-\infty}$  for the given  $A$ , to obtain the value of  $B$  on the whole area.

(ii) The wave equation (14) is solved from  $C|_{y=-\infty}$  with the calculated value of  $B$ , to obtain the value of  $C$  on the whole area.

(iii) By using the value of  $A$  and the value of  $C$  calculated in procedure (ii), the time integration of equation (12) is performed, which gives the value of  $A$  at the next time step.

We adopt the second-order-upwind TVD method [8] to solve the wave equations (13) and (14). Time integration of equation (12) is performed by the Jameson–Baker method [9]. The spatial derivatives in equation (12) are calculated by the fourth-order central discretization. The grid system is generated by standard square lattices and the computational domain is chosen to be sufficiently large. On the main flow  $A$ , we fix the dumping area very near the boundaries to absorb ripples emitted from dromions [6]. We adopt the periodic boundary condition on mean flows  $B$  and  $C$  in the  $x$ -direction because their values decay rapidly to zeros. Practically this scheme needs only one boundary at  $y = -\infty$ .

### 4. Computational results

First, we simulate the exact one-dromion solution in order to see the accuracy of this scheme. In this computation, we take  $k_r = l_r = \frac{4}{5}$ ,  $k_i = l_i = \frac{1}{5}$  and  $\gamma = 3$  as dromion parameters.

We checked the maximum amplitude of  $|A|^2$  and the first conserved quantity of the DS1 equations,

$$I_1 = \int |A|^2 dx dy.$$

The maximum fluctuation of amplitude of  $|A|^2$  is 3% of the total value. These fluctuations are caused when the peak of dromion precisely hits the vertex on the computational domain. The maximum fluctuation of  $I_1$  is  $\Delta I_1/I_1 \sim 10^{-10}$ . From these results, we may say that this scheme is appropriate to calculate dromion solutions.

Our intention is to clarify whether or not dromions propagate stably under the condition that boundaries are driven to move irregularly. We apply two types of movement of boundaries, which are listed in table 1 with figure 1. The interesting one is the case in which we drive boundaries in such a way that the crosspoint of mean flows moves on a circle path. In order to realize this situation, we employ the following boundary conditions for potentials;  $U|_{y=-\infty}$  varying as a function of  $\sin(\omega t)$ , and  $V|_{x=-\infty}$  varying as a function

**Table 1.** Forced movement of boundaries described as the function of  $\sin(\omega t)$  and  $\cos(\omega t)$  in the power index of  $\exp(\eta)$  (equations (6) and (7)).

Name	x-direction ( $\eta_1 + \eta_1^*$ )	y-direction ( $\eta_2 + \eta_2^*$ )	Path of the meanflow crosspoint
Revolution	$k_r(x + \frac{\Omega_r}{k_r} \sin(\omega t))$	$l_r(x + \frac{\omega_r}{l_r} \cos(\omega t))$	Figure (a)
Lissajous	$k_r(x + \frac{\Omega_r}{k_r} \sin(\omega t))$	$l_r(x + \frac{\omega_r}{l_r} \sin(2\omega t))$	Figure (b)

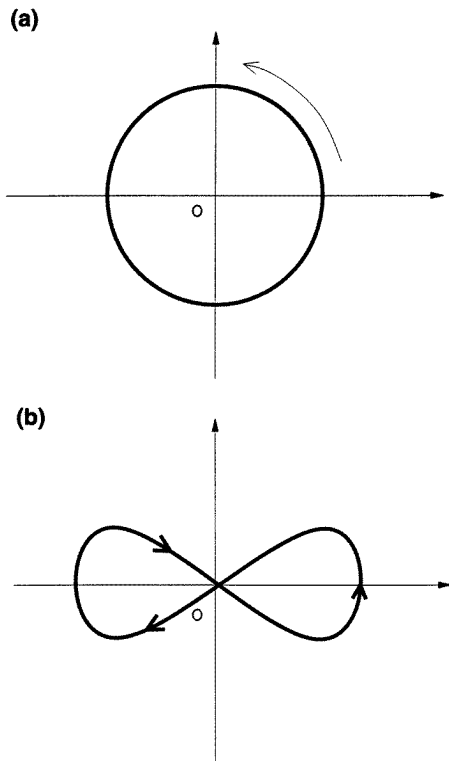


**Figure 1.** Sketches of the motions in table 1. The mean flow crosspoint is driven to move on these curves in the direction indicated by arrows.

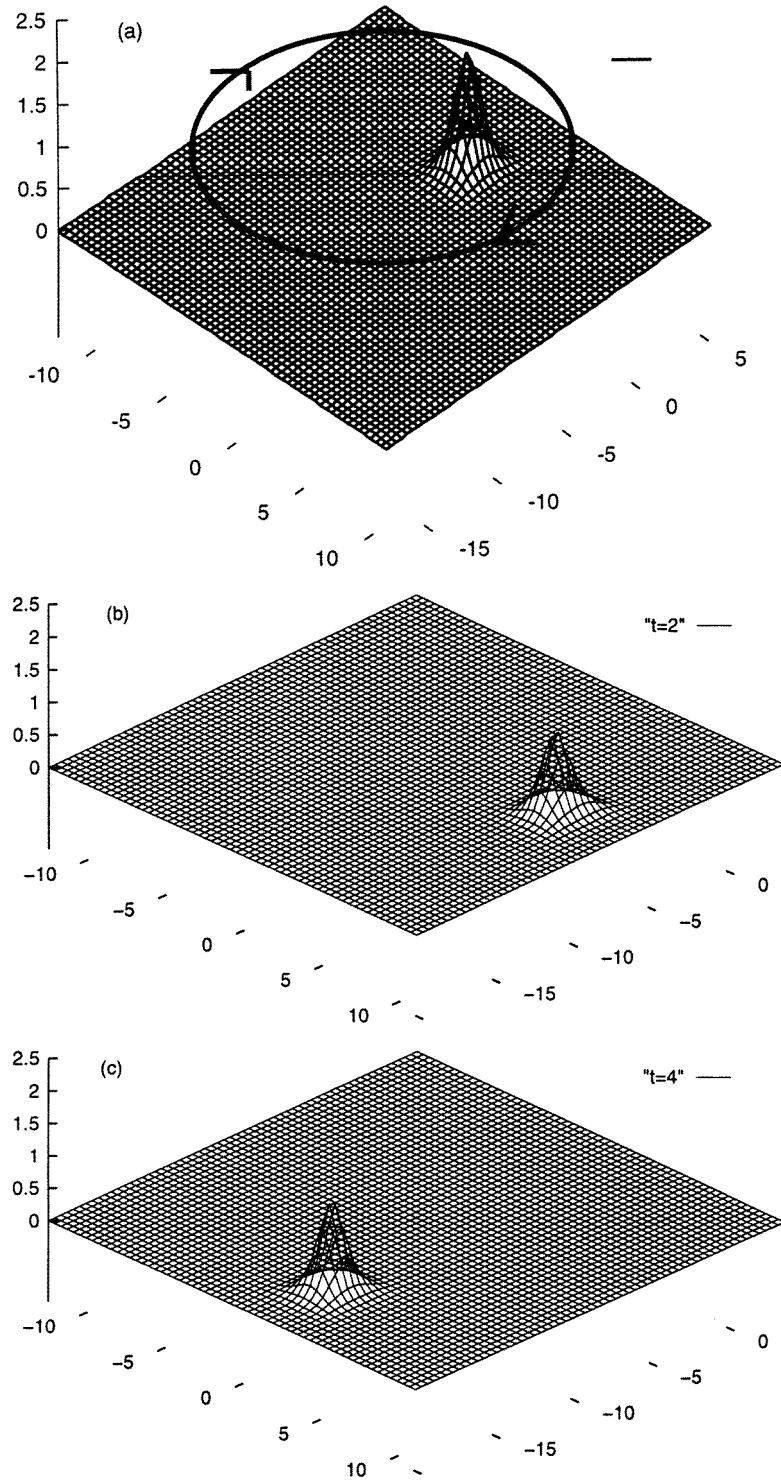


**Figure 2.** Solid profiles of  $|A|^2$  in the case of the revolutionary dromion. (a)  $t = 0.0$ : initial state, (b)  $t = 2.0$ :  $\frac{1}{5}$  rotation, (c)  $t = 4.0$ :  $\frac{2}{5}$  rotation, (d)  $t = 6.0$ :  $\frac{3}{5}$  rotation, and (e)  $t = 8.0$ :  $\frac{4}{5}$  rotation. Dromion is kept localized through the rotation.

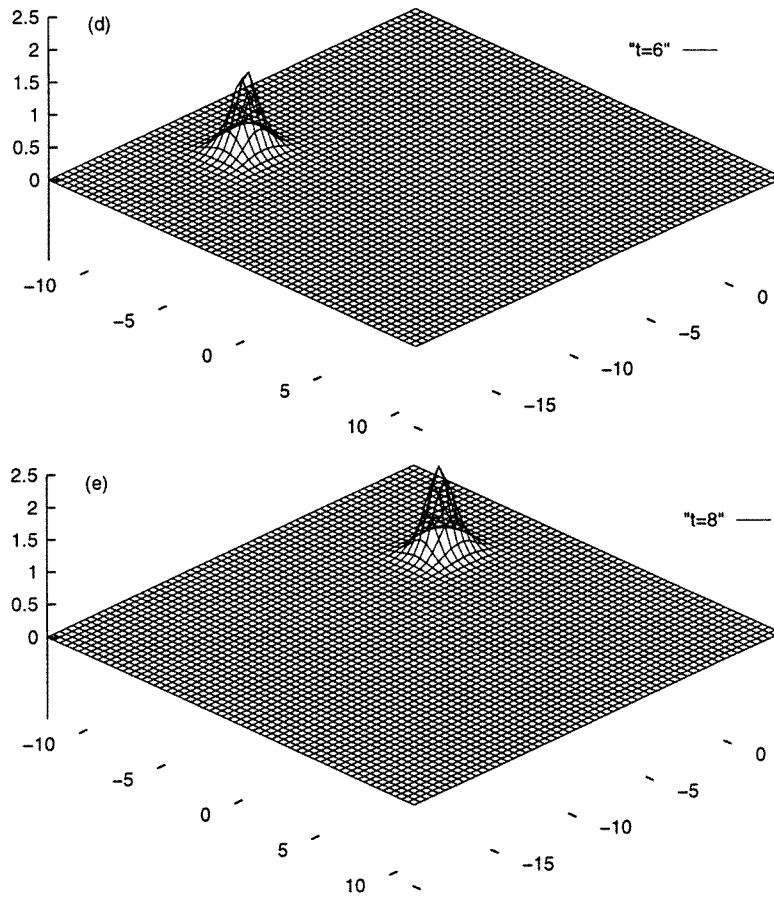


Figure 2. (Continued)

of  $\cos(\omega t)$ . That is, the power index in  $\exp(\eta)$  is replaced by

$$k_r x + \Omega_r t \rightarrow k_r \left( x + \frac{\Omega_r}{k_r} \sin(\omega t) \right) \quad (15)$$

$$l_r y + \omega_r t \rightarrow l_r \left( y + \frac{\omega_r}{l_r} \cos(\omega t) \right) \quad (16)$$

in equations (6) and (7). Then the crosspoint of mean flows rotates around the original point. A simplified sketch is shown in figure 1(a). We shall now discuss the obtained results in detail. Figure 2 shows solid profiles of the main flow. At time  $t = 0$ , both the main flow and the mean flow are set to be exact solutions. Then the mean flow is forced to move at the boundary as explained above. In the results, surprisingly, we see that the dromion keeps its shape and propagates quasistably along the circle. In order to show how much localized volume is preserved and what amount of the original structure is emitted as ripples, the variation of the dromion volume is presented in figure 3. Dromion volume is estimated as,

$$W = \int_s |A|^2 dx dy$$

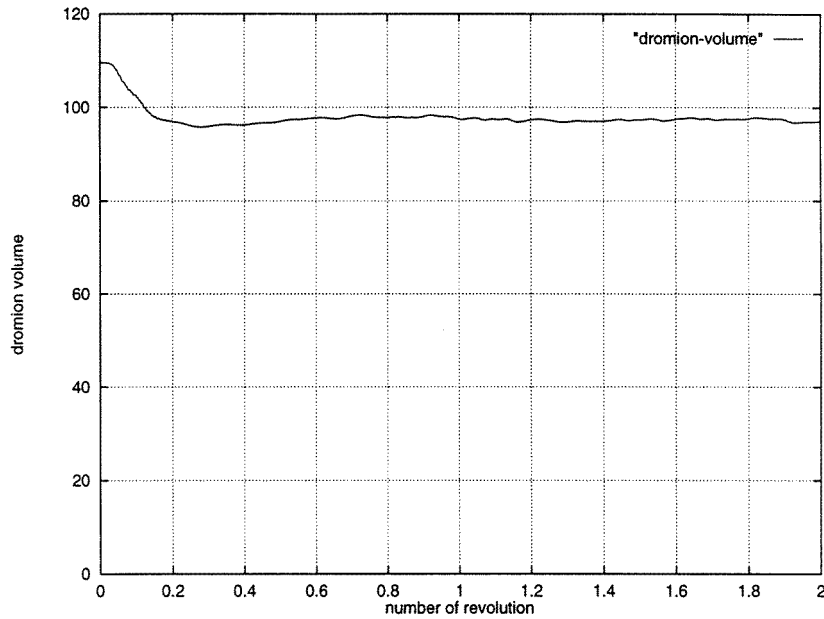


**Figure 3.** Time variation of the volume of the localized structure  $V = \int_s |A|^2 dx dy$ . The horizontal axis is scaled to show the time of revolution.

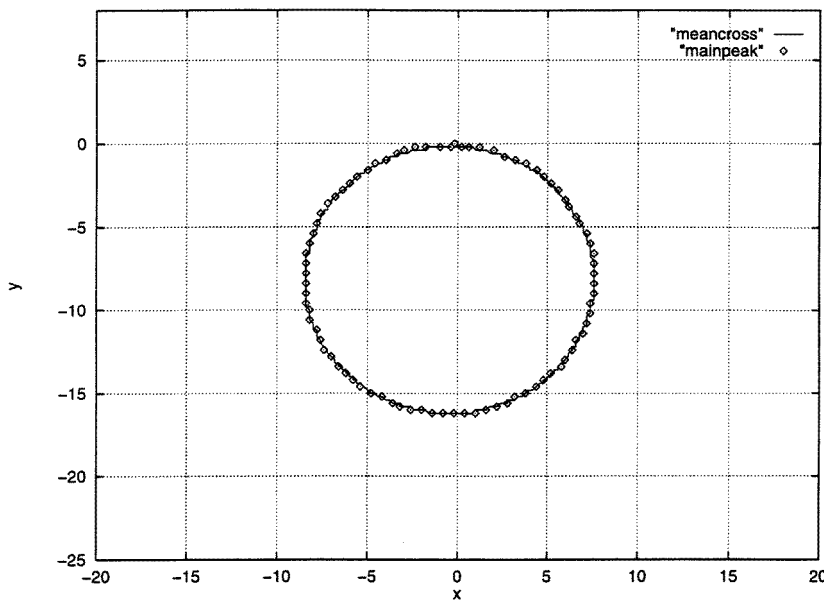


**Figure 4.** Pathline of the mean flow crosspoint. Dots indicate the position of the main flow peak.

where integral domain  $s$  is chosen sufficiently narrow as to contain only the localized structure at the mean flow crosspoint. In figure 3 we can see that the value decreases gradually at the beginning, but then does not change substantially. It is interesting to note



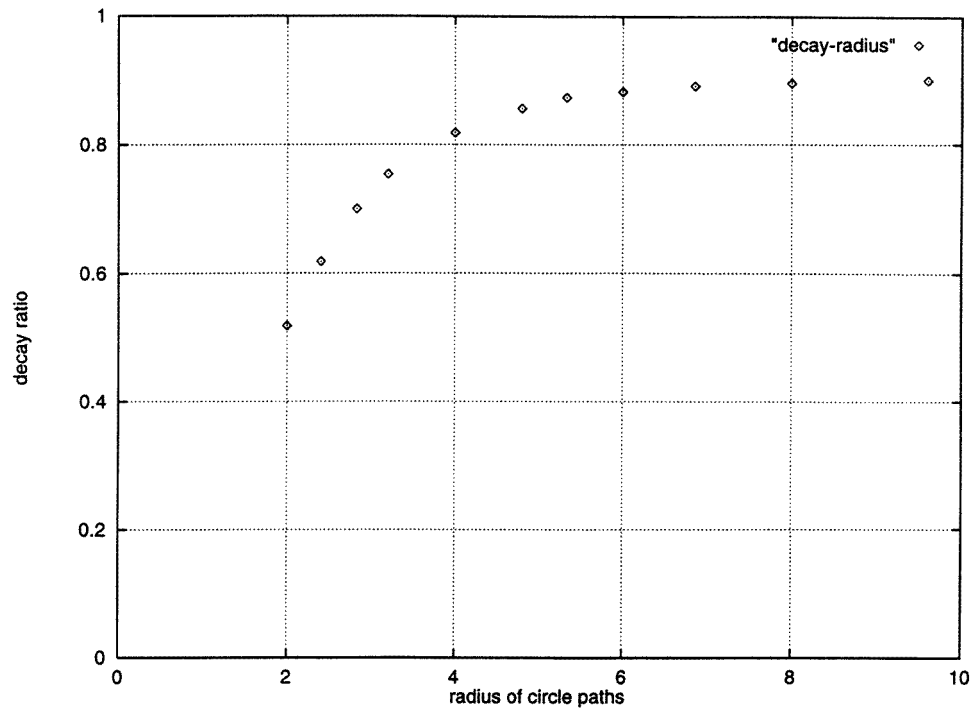


**Figure 5.** Decay ratio of dromion volume versus the radius of the circle. The decay ratio is normalized by the initial volume of dromion. As the radius becomes larger, the decay ratio approaches the value 1.0.

that the dromion volume remains almost steady after it loses some amount. The reason can be explained as follows. In the beginning, the dromion becomes smaller by emitting ripples, which may be caused by the accelerated motion of the mean flow crosspoint. The exact one-dromion propagates at a constant velocity on a straight path, with no acceleration. It keeps its shape and volume perfectly. In the case of revolving dromion, however, it tends to move with the mean flow crosspoint running on a circle path. When dromion is forced to move on any curve, this effect by the crosspoint acts as perturbation. Therefore the balance is broken, which is preserved completely in the case of the exact one dromion, and the dromion reduces its volume, which as a consequence flows away as ripples. Once the dromion reaches a quasistable state, it keeps its shape and propagates almost stably following the motion of the mean flow crosspoint. It should be remarked that the dromion keeps its shape even if it is exposed to the condition apart from the exact solution. We performed computations up to five times revolution and observed that the localized structure always kept its dromion-like shape. Even though the mean flows continues to give perturbation on the dromion, the volume decreases only at the beginning and the system reaches a quasistable state afterwards. Paths of the mean flow crosspoint and the peak of dromion are presented in figure 4. We see that the dromion is completely captured at the mean flow crosspoint. As discussed in the preceding papers, this feature also indicates an important role of the mean flows as an attracting force.

It is likely that the volume of the rotating dromion has a relation to the radius of the mean flow motion. To clarify this relation, we performed several computations keeping the velocity of motion at a constant value. That is, we varied the radius  $r$  and angular velocity

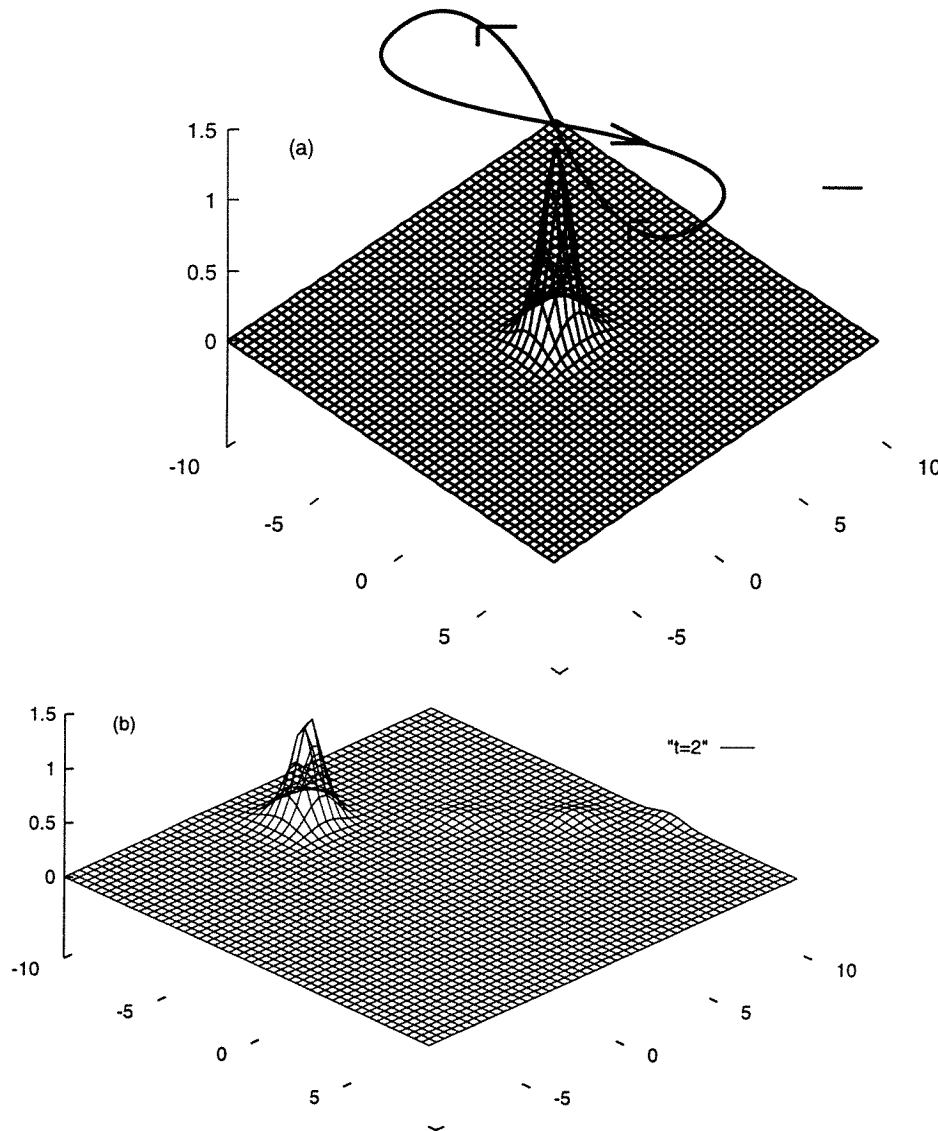


**Figure 6.** Solid profiles of  $|A|^2$  in the case of the Lissajous motion. (a)  $t = 0.0$ : initial state, (b)  $t = 2.0$ :  $\frac{1}{4}$  period, (c)  $t = 4.0$ :  $\frac{2}{4}$  period, (d)  $t = 6.0$ :  $\frac{3}{4}$  period, and (e)  $t = 8.0$ : 1 period. Dromion runs on a Lissajous curve keeping its localized structure.

$\omega$  while keeping  $v = r\omega$  at a constant value. Under this condition, we calculated the decay ratio of the dromion volume after one revolution on a circle path. The relation between the decay ratio and the radius of circle path is shown in figure 5. It can be seen that the ratio of the dromion volume gets closer to the value 1.0 as the radius of the path becomes larger. This feature is reasonable because in the limit  $r \rightarrow \infty$  the system is described by the exact one-dromion solution. In contrast, when the radius becomes smaller, the forced movement of the crosspoint gives a considerable effect on dromion. It emits more ripples and becomes thinner.

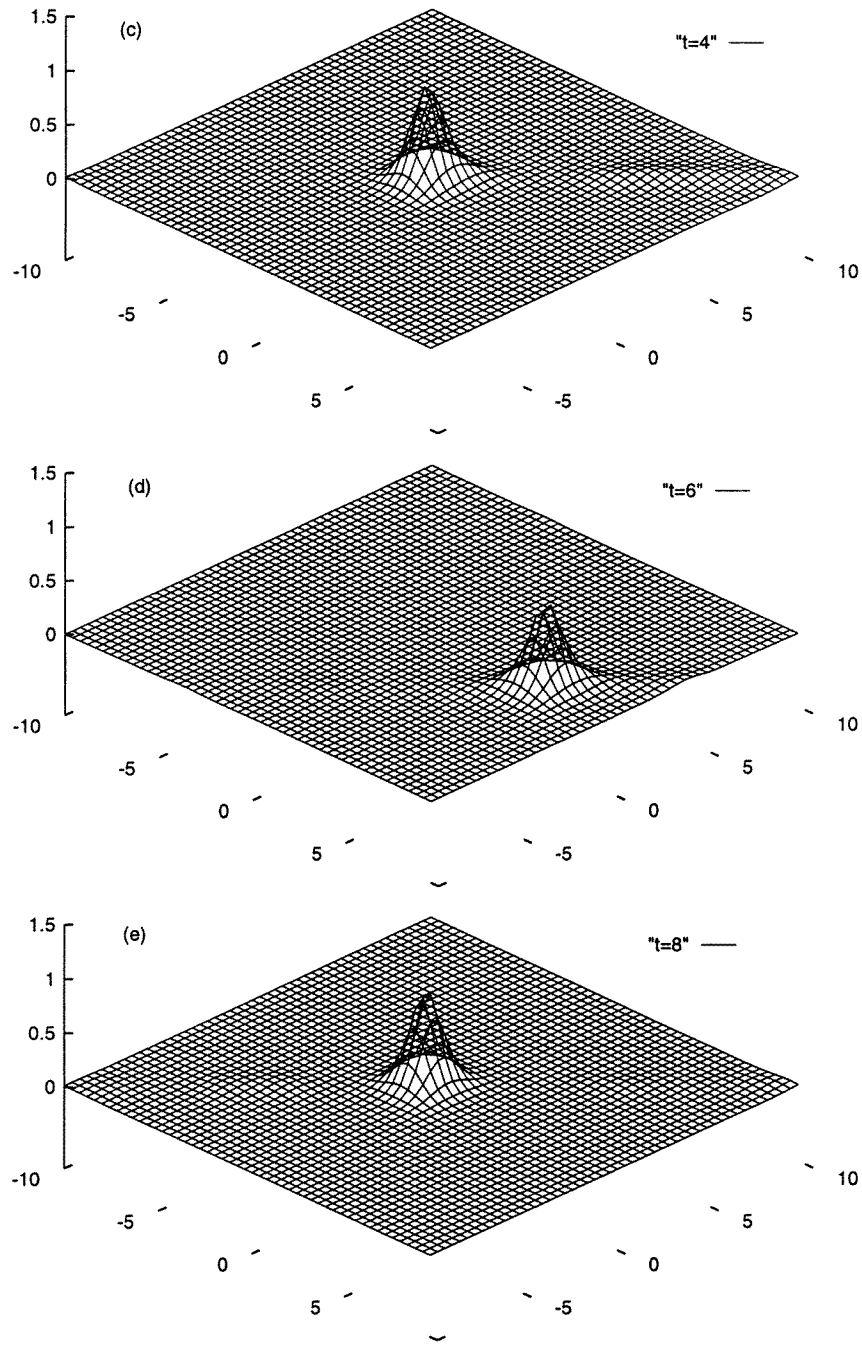
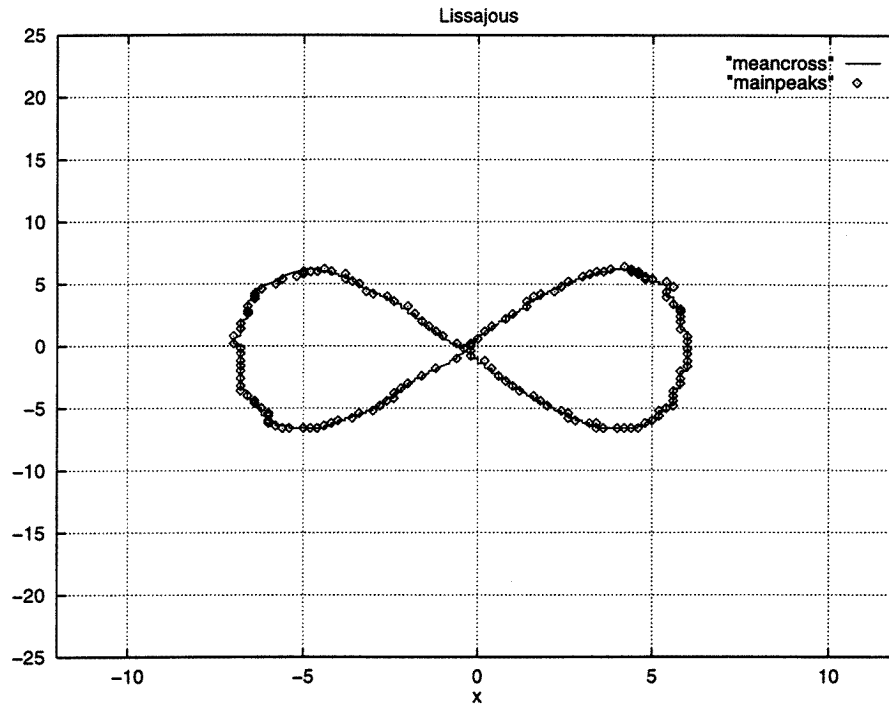


Figure 6. (Continued)



**Figure 7.** Pathline of the mean flow crosspoint. Dots indicate the position of the main flow peak. Both are on the Lissajous curve. The dromion perfectly follows the motion of the mean flow crosspoint.

In order to see whether the change in the orbit of mean flow crosspoint affects the behaviour of dromion or not, we performed a numerical computation in which the crosspoint moves on a Lissajous curve. This situation is realized by replacing  $\cos(\omega t)$  with  $\sin(2\omega t)$  in equation (16). The curve shape is presented in figure 1(b). From figure 6 and also figure 7, we see that the dromion still follows the motion of the mean flow crosspoint and keeps its shape after emitting a certain amount of ripples.

## 5. Concluding remarks

We give two concluding remarks.

(i) A conserved form of the DS1 equations is obtained and a new method for numerical analysis is proposed. By comparing the computational results with the exact solution, the accuracy of the new scheme is proved to be an appropriate one.

(ii) Some behaviours of dromions with driving mean flows at the boundaries are investigated by applying the scheme. Through the calculations, the stable propagation of dromions under particular conditions are observed. It is possible to remote-control dromions from the boundaries by forcing the boundary values to move appropriately.

As for the second conclusion, it has been shown in [5] that an electrostatic ion wave, which propagates perpendicularly to fixed magnetic field, is well described by the DS1 equations. Therefore it is probable that the electrostatic potential of the ion wave is localized in two-dimensional space with the shape of a dromion, and that the mean current of the ion plays a role of the mean flow. In conclusion, if it is possible to control dromions from the

boundaries, there is also the possibility of transporting the energy of the ion wave along a curved path to arbitrary places by arranging the boundary conditions. Moreover, we can estimate the remained volume of dromion in the case that the path is a simple circle.

### Acknowledgments

NY is grateful to Professor Kojiro Suzuki for fruitful discussions and helpful advice. The authors also thank Dr Tetsu Yajima for many valuable comments about DS equations. Special thanks are due to Dr. Lars Söderholm at the Royal Institute of Technology for his comment on this research and to Mr Hirofumi Tomita for providing useful computational tools.

### References

- [1] Ablowitz M J and Segur H 1981 *Solitons and the Inverse Scattering Transform* (Philadelphia, PA: SIAM) p 322
- [2] Boiti M, Leon J J-P, Martina L and Pempinelli F 1988 *Phys. Lett.* **132A** 432.
- [3] Fokas A S and Santini P M 1989 *Phys. Rev. Lett.* **63** 1329
- [4] Davey A and Stewartson K 1974 *Proc. R. Soc. A* **338** 101
- [5] Nishinari K, Abe K and Satsuma J 1994 *Phys. Plasmas* **1** 2559
- [6] Nishinari K and Yajima T 1995 *Phys. Rev. E* **51** 4989
- [7] Nishinari K and Yajima T 1996 *J. Phys. A: Math. Gen.* **29** 4237
- [8] Yee H C 1989 *NASA ARC TM-101088*
- [9] Jameson A and Baker T J 1983 *AIAA Paper* **83**